sible, so this limit can be reduced. As noted earlier when discussing Eq. 1, for molecular collisions in which the masses of the two particles are equal, the contribution of the spread in both beam velocities to the velocity distribution of the scattered molecules vanishes to first order.

The measured RMS velocity spread, 15 m s^{-1}, is greater than three times that predicted by Eq. 4. Our measured velocity spread of cold NO molecules is an upper limit to the actual spread in velocities, as is the temperature associated with this velocity spread. In our experiment, there are several sources that broaden the reported velocity distribution. First is the resolution of the microchannel plate detector and camera, about 8 m s^{-1}. Second, the resolution of the velocity mapping itself can be compromised by charge repulsion of the ions and imperfect ion optics. From measurement of parent ions in our molecular beams, we estimate this to add approximately 10 m s^{-1} of velocity spread. Third is the velocity imparted to the detected NO^+ ions by the recoil of the electron from the NO^+ upon two-photon ionization that creates the NO^+ we detect. The recoiling photoelectron imposes a velocity spread of approximately 10 m s^{-1}. A fourth source of broadening comes from the nature of the measurement, which is a projection of the 3D spherical velocity distribution onto the 2D detector. Scattering above and below the scattering plane gives rise to the asymmetric tail on the distribution of Fig. 3. These sources of broadening in the measured NO velocity distribution account for a substantial fraction of the observed width of the measured distribution.

The vector constraint that must be satisfied to produce zero-velocity molecules, $\mathbf{u}'_{NO} = -\mathbf{v}_{cm}$, can readily be satisfied. It represents two independent scalar constraints in a system in which (for fixed beam intersection angle) there are three experimental variables—the energies of the two colliding molecules and the ratio of their masses—whose values can be selected to achieve that condition. For producing zero-velocity species AB, the AB energy can be adjusted by changing the temperature of the AB free-jet expansion nozzle and the diluent gas in which it is seeded. The energy of the collider species can be selected by the temperature of its free-jet expansion nozzle, and because the chemical identity of the collider species is not important, the ratio of the masses can be readily selected.

References and Notes

1. C. E. Weiman, D. E. Pritchard, D. J. Wineland, *Rev. Mod. Phys.* **71**, S253 (1999).
2. M. H. Anderson, J. R. Ensher, M. R. Matthews, C. E. Wieman, E. A. Cornell, *Science* **269**, 198 (1995).
3. C. C. Bradley, C. A. Sackett, J. J. Tollett, R. G. Hulet, *Phys. Rev. Lett.* **75**, 1687 (1995).
4. K. B. Davis *et al.*, *Phys. Rev. Lett.* **75**, 3969 (1995).
5. S. L. Rolston, W. D. Phillips, *Nature* **416**, 219 (2002).
6. K. Burnett, P. S. Julienne, P. D. Lett, E. Tiesinga, C. J. Williams, *Nature* **416**, 225 (2002).
7. S. A. Diddams *et al.*, *Science* **293**, 825 (2001).
8. A. Kerman, V. Vuletic, C. Chin, S. Chu, *Phys. Rev. Lett.* **84**, 439 (2000).
9. C. Monroe, W. Swann, H. Robinson, C. Wieman, *Phys. Rev. Lett.* **65**, 1571 (1990).
10. W. Ketterle, *Int. J. Mod. Phys.* **16**, 4537 (2002).
11. H. L. Bethlem, G. Meijer, *Int. Rev. Phys. Chem.* **22**, 73 (2003).
12. F. Masnou-Seeuws, P. Pillet, *Adv. Atom. Mol. Opt. Phys.* **47**, 52 (2001).
13. J. T. Bahns, P. L. Gould, W. C. Stwalley, *Adv. Atom. Mol. Opt. Phys.* **42**, 171 (2000).
14. J. P. Shaffer, W. Chalupczak, N. P. Bigelow, *Phys. Rev. A.* **63**, 021401 (2001).
15. H. R. Thorsheim, J. Weiner, P. S. Julienne, *Phys. Rev. Lett.* **58**, 2420 (1987).
16. T. Takekoshi, B. M. Patterson, R. J. Knize, *Phys. Rev. Lett.* **81**, 5105 (1998).
17. J. D. Miller, R. A. Cline, D. J. Heinzen, *Phys. Rev. Lett.* **71**, 2204 (1993).
18. E. A. Donley, N. R. Clausen, S. T. Thompson, C. E. Weiman, *Nature* **417**, 529 (2002).
19. C. A. Regal, C. Ticknor, J. L. Bohn, D. S. Jin, *Nature* **424**, 47 (2003).
20. J. D. Weinstein, R. deCarvalho, T. Guillet, R. Friedrich, J. M. Doyle, *Nature* **395**, 148 (1998).
21. J. Kim *et al.*, *Phys. Rev. Lett.* **78**, 3665 (1997).
22. H. L. Bethlem *et al.*, *Nature* **406**, 491 (2000).
23. H. L. Bethlem, G. Berden, A. J. A. van Roij, F. M. H. Crompvoets, G. Meijer, *Phys. Rev. Lett.* **84**, 5744 (2000).
24. M. Gupta, D. Herschbach, *J. Phys. Chem. A.* **103**, 10670 (1999).
25. M. S. Westley, K. T. Lorenz, D. W. Chandler, P. L. Houston, *J. Chem. Phys.* **114**, 2669 (2001).
26. D. W. Chandler, D. H. Parker, in *Advances in Photochemistry*, D. C. Neckers, D. H. Volman, Eds. (Wiley, New York, 1999), vol. 25.
27. T. J. B. Eppink, D. H. Parker, *Rev. Sci. Inst.* **68**, 3477 (1997).
28. M. S. Elioff, D. W. Chandler, *J. Chem. Phys.* **117**, 6455 (2002).
29. J. Luque, D. R. Crosley, LIFBASE: Database and Simulation Program (v. 1.6), SRI International Report No. MP99-109 (SRI International, Menlo Park, CA, 1999).
30. The error bars reflect uncertainty in our measurement of the mean velocity and are derived by propagation of errors using standard rules. The spread reflects the width of the statistical distribution of velocities in the supersonic molecular beam of NO molecules. We did not measure the speed of the Ar beam; we used the computed value for an ideal isentropic expansion, 554 m s^{-1}, and assumed a spread of 7% FWHM.
31. M. H. Alexander, *J. Chem. Phys*, **111**, 7426 (1999).

32. We thank M. Jaska and B. Parsons for the considerable insight and assistance they provided during the course of this research. Funding for this work was provided by the U.S. Department of Energy, Office of Basic Energy Science, Division of Chemical Sciences, Geosciences, and Biosciences. Sandia is a multiprogram laboratory operated by Sandia Corporation, a Lockheed Martin Company, for the U.S. DOE's National Nuclear Security Administration under contract DE-AC04-94AL85000.

21 August 2003; accepted 6 November 2003

Importance of Surface Morphology in Interstellar H_2 Formation

L. Hornekær,[1*] A. Baurichter,[1] V. V. Petrunin,[1] D. Field,[2] A. C. Luntz[1]

Detailed laboratory experiments on the formation of HD from atom recombination on amorphous solid water films show that this process is extremely efficient in a temperature range of 8 to 20 kelvin, temperatures relevant for H_2 formation on dust grain surfaces in the interstellar medium (ISM). The fate of the 4.5 electron volt recombination energy is highly dependent on film morphology. These results suggest that grain morphology, rather than the detailed chemical nature of the grain surface, is most important in determining the energy content of the H_2 as it is released from the grain into the ISM.

The formation of molecular hydrogen in interstellar molecular clouds is the key first step in both the formation of stars and in the evolution of molecular complexity in the interstellar medium (ISM). It is widely accepted that (i) there is no efficient gas phase route for H_2 formation from H atoms at the low temperatures and densities of the ISM and (ii) H_2 is formed by H atom recombination on dust grains that are integrally associated with the interstellar molecular clouds (*1*). To account for the astronomically observed H_2 formation rate in clouds (*2*, *3*), the surface recombination of H atoms on grains to produce H_2 must be a very efficient process at $T \sim 10$ K (*1*). However, previous laboratory experiments on H_2 formation on surfaces of astrophysical relevance were interpreted as implying that the recombination is thermally activated (*4*), requiring $T \geq 20$ K (*5*) for surfaces thought to be important in dark interstellar clouds. The formation of each H_2 molecule also releases 4.5 eV of energy. How this energy is partitioned amongst the various degrees of freedom is crucial in understanding the temporal and chemical evolution of molecular clouds (*6*). For example, partitioning of the reaction energy into H_2 kinetic energy heats the cloud, while vibrational excitation of the H_2 or

[1]Department of Physics, University of Southern Denmark, Denmark. [2]Department of Physics and Astronomy, Aarhus University, Denmark.

*To whom correspondence should be addressed. E-mail: hornekaer@fysik.sdu.dk

excitation of the grain surface are rapidly (on astronomical time scales) dissipated via radiation that escapes the cloud. Thus, the time scale for collapse of a cloud to yield cores of high density where stars ultimately form depends critically on the energy disposal in H_2 formation (*6*). In addition, if a large fraction of the 4.5 eV goes into local heating of the grain, this can thermally catalyze other chemical reactions on the grain and/or desorb other atoms or molecules adsorbed in close vicinity on the grains (*7*). Unfortunately, at present no definitive aspects of this energy partitioning can be directly inferred from observational astronomy.

The chemical nature of the dust grains is not well characterized, but astronomical data and studies of meteorites show that they are principally composed of silicate and carbonaceous material. In diffuse (low density) clouds, the dust grains are bare, but in dark (dense) clouds, the grains are covered with "ice" mantles, principally amorphous solid water with added CO, CO_2, methanol, and other molecules (*8*, *9*). Though the size distribution of the interstellar grains is accepted to follow a power law, their morphology is not well determined. Hence, it is unknown whether the typical ~0.1 μm diameter particles thought to be important in the formation of H_2 in the ISM are solid compact particles, porous structures, open fractal-like structures, or other possible modifications.

Here, we present laboratory experiments on H+D recombination that simulate the formation of H_2 in the ISM. On amorphous solid water (ASW) films, which are believed to be good analogs for ice mantles on interstellar grains in dark clouds (*9*), we find a very efficient recombination mechanism that occurs at surface temperatures as low as 8 K and that implies fast mobility of H and D atoms at this temperature. In porous ASW films, the major fraction of HD produced is subsequently retained as a physisorbed molecule in the pores and is not released into the gas phase until the film is externally heated above the HD molecular desorption temperature. In this case, most of the 4.5 eV recombination energy is lost to the ASW film. On nonporous ASW films, however, the experimental results show minimal retention of the HD formed by atom recombination on the surface of the ASW film. This result implies prompt ejection of the HD formed into the gas phase with its nascent energy distribution. Theory indicates that the nascent reaction energy is principally partitioned into HD internal and translational excitation (*10*). Thus, the overall mechanism for formation of gas phase HD and its energy distribution depends critically on film morphology. We argue that this same dependence on morphology should exist for H_2 formation on ice-covered grains in dense interstellar clouds. In addition, we suggest that the dependence of the H_2 energy distribution on grain morphology should also apply for H_2 formation on bare grains in diffuse clouds, so that the dominant effect controlling the energy of H_2 formed throughout the ISM may not be the detailed chemical nature of the grain surfaces but rather their morphology.

In our experiments, ASW films are grown on a Cu substrate attached to a flowing liquid He cryostat by depositing H_20 onto the substrate from a capillary array "doser" (*11*). Under our H_2O deposition conditions and a surface temperature $T_s \leq 10\ K$, modestly porous ASW films are grown [$\xi_{por} \cong 0.05$, where ξ_{por} is defined as the percentage increase in internal surface area per monolayer (ML) of ASW relative to the external surface area of the film] (*12*). With H_2O deposition at T_s = 120 K, nonporous ASW films are grown (*12*). HD formation is induced by exposing the films to separate H and D atomic beams (*13*) that spatially overlap at the center of the ASW surface in an ultra–high vacuum chamber ($\leq 10^{-10}$ torr). After dosing with H+D beams, we perform both temperature programmed desorption (TPD) measurements and laser induced thermal desorption (LITD) measurements (*14*).

The TPD spectrum of HD resulting from H+D recombination on porous ASW exhibits a large signal peaking at a temperature of 28 K (Fig. 1A). Turning off either or both discharges producing H and D atoms causes the large HD TPD peak to disappear; therefore, the signal arises from recombination of H and D atoms on the external or internal (pore) surfaces of the ASW film. The dashed line (Fig. 1) shows the TPD spectra for D_2 after only molecular D_2 dosing. HD molecules formed by atom recombination on the ASW films are desorbed at the same temperature as D_2 molecules that are adsorbed molecularly. In equivalent experiments for dosing on a nonporous ASW film (Fig. 1B), the intensity of the HD TPD signal is extremely weak.

We show elsewhere (*15*) that in the low D_2 coverage limit, there is a substantial increase in the TPD peak temperature with increasing thickness of porous ASW films and a strong sensitivity of the TPD spectra to thermal annealing, which reduces porosity. The origin of this phenomenon is attributed to fast diffusion of the D_2 molecules producing a uniform distribution of adsorbed molecules on the total surface of the ASW film (both pore walls and external surface). During the TPD ramp, molecules adsorbed on the pore walls undergo a random walk of desorption-readsorption cycles until they reach the outer surface and desorb into the gas phase. This cycling causes the TPD peak for D_2 to appear at substantially higher temperatures for the porous ASW relative to the nonporous ASW film (*16*). The dependence of the TPD spectra on both porous ASW film thickness and thermal annealing for HD formed by H+D recombination is identical to that for D_2 from molecular dosing.

The observation that the HD formed by atom recombination always desorbs at the same temperature as D_2 molecularly dosed onto the surface irrespective of the film thickness or thermal history suggests that H and D atoms are mobile on the film surface at temperatures below the molecular desorption temperature and undergo a Langmuir-Hinshelwood or hot atom (*17*) recombination to form HD, which is then retained in the pores until the temperature is externally ramped to a high enough temperature to cause molecular desorption. This retention of the formed molecules was seen to be efficient for an ASW film thickness as low as 30 monolayers. To determine the temperature at which the atoms become mobile and recombine, sequential dosing of D and H atoms was compared to simultaneous H+D dosing for porous ASW (Fig. 2). Even at 8 K, sequential dosing leads to a large decrease of HD intensity in the TPD relative to that for simultaneous dosing. Simultaneous dosing, followed by extended waiting periods (30 min), showed no decreases in HD intensity, implying that the decrease was not due to desorption of atoms or HD during the waiting period. The results imply fast recombination either via the Langmuir-Hinshelwood or hot atom mechanism, i.e., that the isotope dosed initially recombines forming D_2 or H_2 molecules and that this process leaves no free atoms to react when the second isotope is dosed later (*18*). Thus, these results show that even at 8 K the atoms are mobile enough to recombine. Because of the small intensity of the HD desorption peak on nonporous ASW, it was not possible to do similar experiments on this surface. However, there is no reason to suspect that surface atom mobility is less on the nonporous surface than on the porous ASW. We believe that these experiments rule out an interpretation that the major route to HD formation on ASW requires thermally activated H atom diffusion to induce a Langmuir-Hinshelwood recombination at temperatures above 20 K, as has been suggested previously (*5*).

The overall efficiency of the molecular HD formation process on a surface is expressed as

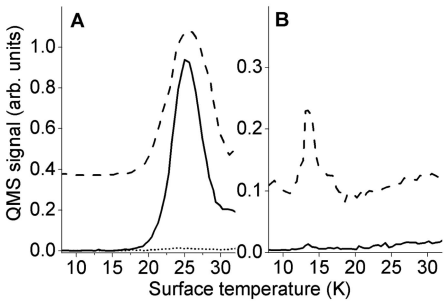

Fig. 1. (**A**) HD QMS signal during TPD after a 10 min dose of H+D (solid line), after a 10 min dose of H_2 + D_2 (dotted line), and D_2 QMS signal after a 10 min dose of D_2 (dashed line) onto a ~2000 monolayer (ML) porous ASW film. The D_2 QMS signal has been offset for clarity. (**B**) HD QMS signal during TPD after a 5 min dose of H+D (solid line) and D_2 QMS signal after a 5 min dose of D_2 (dashed line) onto a ~300 ML nonporous ASW film. The D_2 QMS signal has been offset for clarity.

$S\eta$, where S is the sticking probability of the H or D atom on the surface (assuming they are equal), and η is the probability of an adsorbed atom recombining with another adsorbed atom on the surface. Because we measure the HD in TPD, we only measure the fraction of HD formed by recombination that is retained in the porous structure by adsorption on the internal pore surfaces of the film and is then subsequently desorbed thermally during the TPD. Denoting this fraction as μ implies that the integrated HD TPD intensity is proportional to $\mu S\eta$. We determine absolute values of $\mu S\eta$ using a single D atom beam for relative measurements combined with a single D_2 sticking measurement for absolute scaling. By comparing the integrated D_2 TPD intensity obtained when dosing with discharge on (D atoms + residual D_2 beam) to that obtained when dosing with discharge off (D_2 only) and knowing the extent of dissociation in the beam, we obtain $\mu S_D\eta/S_{D2}$, where S_D is the sticking probability for D atoms and S_{D2} is the sticking probability for D_2 molecules. Measurement of S_{D2} (*19*) gives the absolute measurements for $\mu S_D\eta$ shown in Fig. 3. $\mu S_D\eta$ is large (~0.35) on porous ASW and decreases slightly at $T_s \geq 17$ K, but it is nearly zero (within experimental error) on nonporous ASW. The same results were obtained qualitatively by measuring the HD intensity in TPD with simultaneous dosing of H and D atoms; i.e., the retained fraction of HD for nonporous ASW is minimal relative to that for porous ASW (Fig. 1), and the HD production drops off gradually at $T_s \geq 17$ K for porous ASW. The decrease in $\mu S_D\eta$ with T_s is ascribed to thermal desorption of atoms competing with their recombination, i.e., to a decrease in η with T_s. For pure physisorption systems (such as D and D_2 interacting with ASW), we anticipate that $S_D \leq S_{D2}$ because of the increased elastic scattering of the D atom relative to D_2 (*20*) such that $\mu\eta \geq 0.6$ for porous ASW (*19*) and $\mu\eta \sim 0$ for nonporous ASW. Because there is no reason to suspect that $\eta \leq 1$ at low T_s for either film, we interpret these results as implying that $\mu \geq 0.6$ for porous ASW and $\mu \sim 0$ for nonporous ASW. Thus, prompt desorption dominates for nonporous ASW films, whereas retention in the films dominates for the porous ASW.

A direct measurement of the kinetic energy of the desorbing HD molecules formed by H+D recombination on the porous ASW surface (Fig. 4A) and of molecularly adsorbed D_2 (Fig. 4B) was obtained from LITD and time of flight (TOF) data. A peak temperature of 45 ± 10 K is estimated for the laser-induced temperature jump (*21*). The smooth curves on the figure give the LITD signal anticipated for thermal desorption from a surface at this temperature. Similar kinetic energy distributions are obtained both for HD formation by H+D and in molecular D_2 adsorption, and both are nearly equivalent to that anticipated from thermal desorption at the peak temperature of the laser-induced temperature jump. Therefore, we infer that all of the nascent kinetic energy from H+D formation is lost to the porous ASW before desorption into the gas phase.

On the basis of the observations presented above, the following picture of HD formation on ASW emerges: H and D atoms are mobile and efficiently recombine even at temperatures as low as 8 K. For porous ASW, the dominant fraction of the recombination occurs within the pores at the surface of pore walls. Once formed, the HD is retained in the porous structure until molecular desorption thermally occurs. This is induced to occur on a reasonable laboratory time scale by raising the temperature by an external temperature ramp. Upon initial HD formation, 4.5 eV energy is released into both internal and translational energy of the HD, as well as some small amount into the lattice. The fraction partitioned into kinetic energy is dissipated in collisions with the pore walls as the HD molecularly adsorbs. Similarly, because nonradiative vibrational and rotational relaxation times for molecules physisorbed on surfaces are less than milliseconds (*22*, *23*), especially on H_2O surfaces, any vibrational or rotational excitation produced in HD formation will also be fully relaxed before molecular desorption. Thus, the HD formed in the recombination desorbs in thermal equilibrium with the surface, having lost essentially all of the 4.5 eV recombination energy to the ASW film before desorption. The possible minor fraction of molecules that is not retained in the pores due to recombination on or near the external surface ($1 - \mu < 0.4$) will presumably desorb with only a partially thermalized energy distribution whose details will depend on details of the path of the HD after formation to the external surface. For the nonporous ASW, we observe that $\mu \sim 0$, so the dominant fraction of formed HD desorbs with its nascent energy distribution, i.e., according to present theory with high internal and translational excitation of the HD (*10*). Thus, energy partitioning of the 4.5 eV exoergicity between HD excitation and the ASW depends critically on the morphology of the ASW film.

Because grains in dark clouds are believed to have ice mantles with a major component comprised of ASW, the conclusions from the laboratory experiments reported here should be directly relevant to the mechanism and energy partitioning in H_2 formation in dark clouds. Thus, if the ASW film on the grain is porous, either because the underlying bare grain is highly porous or the ASW film grown on a compact grain is porous, then most (fraction μ) of the H_2 formed will be retained in pores of the grain until it is desorbed thermally at a rate of approximately 10^{-7} s^{-1} at 10 K. Although this rate is slow by laboratory standards (and thus we only observe thermal desorption at higher temperatures in the experiments), this still implies thermal desorption in an astronomically short time (i.e., less than a year). Thus, most of the recombination energy will be deposited into the grain without much excitation of H_2 in the gas phase being produced. Alternatively, for H_2 formation on compact grain mantles, $\mu \sim 0$ and theory then predicts that most of the gas phase H_2 is produced with nearly the full recombina-

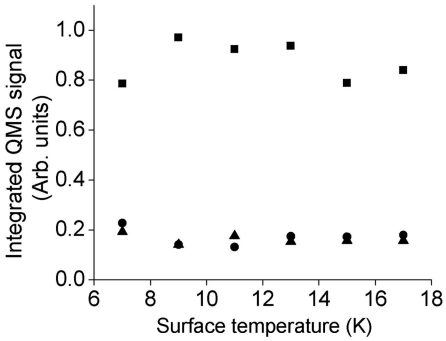

Fig. 2. Integrated HD TPD (QMS) signal after H+D dosing on a ~ 2000 ML porous ASW film versus surface temperature during the atom deposition for the following dose conditions: (■) 5 min simultaneous dose of H+D; (●) 5 min dose of D atoms followed by a 2 min wait period and then a 5 min H atom dose; and (▲) 5 min dose of H atoms followed by a 2 min wait period and then a 5 min D atom dose.

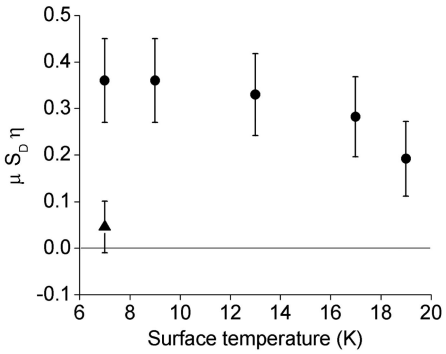

Fig. 3. Recombination efficiency, $\mu S_D\ \eta$, into retained D_2 on a ~2000 ML porous ASW film (●) and (▲) on a ~2000 ML nonporous ASW film.

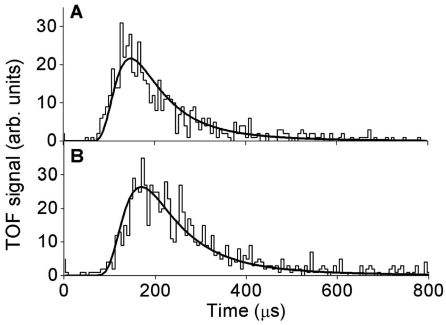

Fig. 4. TOF spectra from a ~200 ML porous ASW film after (**A**) 10 min H+D dose and (**B**) 10 min D_2 dose. The smooth curves are simulated TOF spectra expected for molecules coming off a 45 K surface with a thermal Maxwell-Boltzman velocity distribution.

tion energy partitioned into H_2 excitation (*10*). In diffuse clouds H_2 formation is thought to occur on the surface of bare carbonaceous and silicate grains. Recent experiments on the formation of interstellar carbon dust grain analogs suggest that these could very well be microporous structures showing nanometer-scale porosity (*24*). Because H and H_2 are physisorbed on these surfaces (and internal pore surfaces) with similar binding energies to that of ASW, and energy transfer mechanisms between H_2 and the pore surfaces are likely similar (*16*), we suggest that H_2 retention in pores will be similar on the bare grains to that for ASW. Hence, the energy distribution in H_2 formation could show a similar dependence on dust grain morphology for bare carbonaceous grains as seen here for ASW films. All that is required is that the morphology (pore structure) induces a lifetime on the grain that is long compared with the overall energy relaxation time for the nascent H_2 exoergicity. For silicates, both compact and fluffy grain particles have been found in meteorites and have been grown under laboratory conditions relevant to the ISM. However, the details of the morphology of these grains is unknown, so we can only speculate that the energy budget of H_2 produced on these grains should depend in a similar way to internal morphology as for the ASW films. Therefore, we propose that the dominant effect controlling the initial energy distributions of gas phase H_2 formed in the ISM may not be the detailed chemical nature of the grain surfaces but rather their morphology.

References and Notes

1. D. Hollenbach, E. E. Salpeter, *Astrophys. J.* **163**, 155 (1971).
2. M. Jura, *Astrophys. J.* **197**, 575 (1975).
3. C. Gry *et al.*, *Astron. Astrophys.* **139**, 675 (2002).
4. N. Katz, I. Furman, O. Biham, V. Pironello, G. Vidali, *Astrophys. J.* **522**, 305 (1999).
5. G. Manico, G. Raguni, V. Pironello, J. Roser, G. Vidali, *Astrophys. J.* **548**, L253 (2001).
6. D. R. Flower, G. P. des Forêts, *Mon. Not. R. Astron. Soc.* **247**, 500 (1990).
7. W. W. Duley, D. A. Williams, *Mon. Not. R. Astron. Soc.* **260**, 37 (1993).
8. J. M. Greenberg, *Surf. Sci.* **500**, 793 (2002).
9. E. L. Gibb, D. C. B. Whittet, W. A. Schutte, *Astrophys. J.* **536**, 347 (2000).
10. J. Takahashi, K. Masuda, M. Nagaoka, *Astrophys. J.* **520**, 724 (1999).
11. H_2O deposition conditions are typically ~45° HWHM angular spread and 0.3 to 3 ML/s dose rates.
12. K. P. Stevenson, G. A. Kimmel, Z. Dohnalek, R. S. Smith, B. D. Kay, *Science* **283**, 1505 (1999).
13. The triply differentially pumped H and D atom beams are formed by microwave discharges with fluxes of $\leq 10^{13}$ atoms cm^{-2-1}, beam dissociation probabilities of ~65%, and Maxwell-Boltzmann kinetic energy distributions of $T = 300$ K. The H and D beams are incident upon the ASW surface at 0° and 4° relative to the surface normal and are overlapped at the center of the ASW surface with beam diameters of 1.5 mm and 3.5 mm, respectively.
14. TPD measurements are performed by heating the sample with a linear ramp (typically 0.5 K/s) using electron bombardment on the back side of the Cu substrate and simultaneously detecting the desorption of HD, H_2, and D_2 from the front of the ASW surface with a differentially pumped quadrupole mass spectrometer (QMS) with an aperture close to the ASW surface to limit the field of view in the TPD. LITD measurements were performed by inducing a temperature jump of typically 20 ns on the surface using a 200 μJ laser pulse at 532 nm focused to a 1.5 mm diameter spot at the center of the overlapped atom beams. The kinetic energy distribution of molecules desorbing during the temperature jump are obtained from the TOF distributions to another differentially pumped mass spectrometer placed 10 cm from the surface (*21*).
15. L. Hornekær, A. Baurichter, V. Petrunin, B. Kay, A. Luntz, in preparation .
16. The desorption yield and TPD spectra for HD were unaffected by repeated cycling of H+D adsorption experiments on the same ASW film, indicating that little restructuring of the ASW pore structure takes place as a result of the release of the recombination energy. Hence, the retainment of HD molecules in ASW pores is not caused by pore collapse and volcano formation, as seen for more tightly bound adsorbates exhibiting rapid low-temperature thermal diffusion (*25*), but is simply due to the fact that particles desorbing from pore surfaces in the porous network have to undergo a series of adsorption-desorption cycles before making their way to the external film surface, from which desorption into the gas phase can take place.
17. The distinction between the Langmuir-Hinshelwood (LH) and hot atom reaction mechanisms is in the origin of atom mobility on the 10 K surface. In the LH mechanism, this is caused by thermal atom diffusion, whereas in the hot atom mechanism this is caused by transient mobility on the surface during the adsorption process, i.e., before the atom fully thermalizes on the surface. All experiments reported here are consistent with both mechanisms. Our bias is that the LH mechanism dominates because of the absence of H coverage dependence in apparent rates of recombination and because it is hard to rationalize HD retention in the internal porous surface if hot atom reaction occurs on the external surface.
18. The small residual signal in Fig. 2 is thought to arise from recombination of atoms trapped at the Cu-substrate–ASW interface.
19. $S_{D2} = 0.6 \pm 0.10$ for porous ASW and $S_{D2} = 0.20 \pm 0.15$ for nonporous ASW at $T_s \sim 8$ K, as obtained by the King and Wells method.
20. S. Andersson, L. Wilzen, M. Persson, J. Harris, *Phys. Rev. B* **40**, 8146 (1989).
21. L. Diekhöner, H. Mortensen, A. Baurichter, A. C. Luntz, *J. Chem. Phys.* **115**, 3356 (2001).
22. H. C. Chang, G. E. Ewing, *J. Electron Spectrosc.* **54**, 39 (1990).
23. M. Bonn, M. J. P. Brugmans, A. W. Kleyn, R. A. van Santen, *Chem. Phys. Lett.* **233**, 309 (1995).
24. M. Schnaiter *et al.*, *Astrophys. J.* **519**, 687 (1999).
25. M. P. Collings, J. W. Dever, H. J. Fraser, M. R. S. McCoustra, D. A. Williams, *Astrophys. J.* **583**, 1058 (2003).

26. Supported by The Danish National Research Council (grant no. 21000269), the Danish National Research Foundation through the Aarhus Center of Atomic Physics, and the Carlsberg Foundation. We thank B. Kay and A. Andersen for useful discussions and advice.

26 August 2003; accepted 11 November 2003

Fault Interactions and Large Complex Earthquakes in the Los Angeles Area

Greg Anderson,*† Brad Aagaard,‡ Ken Hudnut

Faults in complex tectonic environments interact in various ways, including triggered rupture of one fault by another, that may increase seismic hazard in the surrounding region. We model static and dynamic fault interactions between the strike-slip and thrust fault systems in southern California. We find that rupture of the Sierra Madre–Cucamonga thrust fault system is unlikely to trigger rupture of the San Andreas or San Jacinto strike-slip faults. However, a large northern San Jacinto fault earthquake could trigger a cascading rupture of the Sierra Madre–Cucamonga system, potentially causing a moment magnitude 7.5 to 7.8 earthquake on the edge of the Los Angeles metropolitan region.

Faults interact with each other over a variety of temporal and spatial scales. Long-term interactions through static stress transfer have been observed in Turkey, Alaska, California, Japan, and elsewhere, whereas dynamic rupture propagation from one fault to another during a single event has been seen in several recent large earthquakes (*1–3*). Although these studies have largely concentrated on strike-slip faults, some large events—including the 1957 moment magnitude (M_w) = 8.3 Gobi-Altay (*4*) and 2002 M_w = 7.9 Denali Fault, Alaska (*5*, *6*), earthquake sequences—involved interactions between thrust and strike-slip fault systems. Many heavily populated regions contain thrust and strike-slip fault networks, so understanding the mechanisms by which faults in such networks interact is critical for improved estimates of seismic hazard and risk in those areas.

The northern edge of the densely populated Los Angeles metropolitan region is bounded by the Sierra Madre–Cucamonga (SMF-CF) thrust fault system, which produced the M_w = 6.7 1971 San Fernando earthquake and may generate events up to M_w = 7.5 (*7*). To the east and north lie the San Andreas (SAF) and San Jacinto (SJF) right-lateral strike-slip fault systems; each may slip in events exceeding M_w = 7.0, and events of M_w = 7.8 occurred on the SAF in 1685 and 1857 (*8*). Here, we examine

U.S. Geological Survey, 525 South Wilson Avenue, Pasadena, CA 91106–3212, USA.

†Present address: UNAVCO, 6350 Nautilus Drive, Boulder CO 80301, USA.

‡Present address: U.S. Geological Survey, 345 Middlefield Road, M/S 977, Menlo Park CA 94025, USA.

*To whom correspondence should be addressed. E-mail:anderson@unavco.org